

## Electrochemical Impedance Spectroscopy Behavior of Nanometric Al-Cr and Cr-Al Coatings by Magnetron Sputtering

C. P. Castillo Morquecho<sup>1</sup>, C. López Meléndez<sup>1</sup>, M.I. Flores-Zamora<sup>2</sup>, R.G. Bautista-Margulis<sup>3</sup>, H. E. Esparza Ponce<sup>1</sup>, F. Almeraya Calderón<sup>1,4</sup>, C. Gaona Tiburcio<sup>4</sup>, A. Martínez-Villafañe<sup>1,\*</sup>

<sup>1</sup> CIMAV-Chihuahua. Miguel de Cervantes 120, Complejo Industrial Chihuahua. C.P. 31109

<sup>2</sup> Universidad Juárez Autónoma de Tabasco, División Académica de Ciencias Biológicas, Villahermosa, Tab., 86040, México.

<sup>3</sup> Universidad Autónoma de Chihuahua, Facultad de Ingeniería. Chihuahua, Chih. México

<sup>4</sup> Universidad Autónoma de Nuevo León, FIME – Centro de Innovación e Investigación en Ingeniería Aeronáutica, Av. Universidad s/n, Ciudad Universitaria, San Nicolás de los Garza, Nuevo León, Mexico

\*E-mail: [martinez.villafane@cimav.edu.mx](mailto:martinez.villafane@cimav.edu.mx)

Received: 30 November 2011 / Accepted: 12 January 2012 / Published: 1 February 2012

---

Multilayer and bilayers structures have attracted much attention as a way of improving the mechanical and corrosion resistance properties of protective coatings. In this work the application of nanometric Al/Cr and Cr/Al bilayers deposited on AA2024-T3, AA60601-T6 aluminum alloys and AISI 9840 steel by magnetron sputtering and DC sputtering was studied. The materials were characterized by scanning electron microscopy (SEM), atomic force microscopy (AFM), transmission electron microscopy (TEM), X-ray diffraction (XRD) and electrochemical impedance spectroscopy (EIS) in order to consider their application as high corrosion resistance coatings. The corrosion behavior of the films was studied using a NaCl aqueous solution (3.5 wt %)

---

**Keywords:** Nanometric films, DC Magnetron Sputtering, Coatings, EIS

### 1. INTRODUCTION

Aluminum alloys have a wide diversity of industrial applications because of their light weight, high electric conductivity, and corrosion resistance. Generally, they are used more often than any other metal, except steel [1]. Aluminum, when alloyed with small amounts of other materials, is an essential and valuable metal because of its high specific strength and low density. However, untreated Al-Mg-Cu based alloys like AA2024, AA6061 and AA7075 are susceptible to corrosion [2]. Aluminum

coatings are used on an industrial scale and can be applied by using a variety of methods including metal spraying, hot dipping or cladding. Where fine tolerances are required, aluminum coatings can be deposited by electrodeposition from organic electrolytes [3] or, more usually, by ion-vapor deposition (IVD) or other vacuum techniques [4]. Since the early 1970s aluminum coatings deposited by the IVD route have been produced commercially and the technology required to obtain controlled thicknesses on both simple and complex shapes is well established. Aluminum coatings are now routinely employed for corrosion protection, decoration of metallic and non-metallic surfaces and have been suggested as a means of cladding less corrosion resistant aluminum alloy substrates [5]. Aluminum coatings are used for the corrosion protection of ferrous substrates for two main reasons. Firstly, aluminum with its air-formed passive oxide film forms an effective barrier layer against attack and, secondly, if the underlying substrate is exposed at, for example, the base of pre-existing defects or corrosion pits, the aluminum coating will afford a degree of sacrificial protection to the substrate. Furthermore, industry demands advanced materials and technology for the preparation of these materials, which include aerospace, automotive, and defense applications. The search for new methods and processing techniques for improving certain material properties of these alloys has gained great importance in recent decades [6]. Conversion layers have been studied as a promising alternative to protect Iron and aluminum alloys. Many works have been published about different methods and conditions to obtain Al-Cr conversion layers on several steel and aluminum alloys substrates that are of interest to the aircraft industry and their microstructure and corrosion behavior have been investigated [7–13]. Transition metals are added to compensate for the low mechanical properties of pure aluminum. A good thermal stability, due to the low solubility and diffusivity of Cr in aluminum, is expected. The similarities, in terms of microstructure and corrosion resistance, of the Al-Cr and Cr-Al systems are pointed out.

## 2. EXPERIMENTAL

Samples of AISI9840 Steel and AA2024-T3 and AA6061-T6 aluminum in the form of squares (AISI9840 and AA6061-T6) and discs (AA2024-T3) were ground up to 1000-grade SiC paper, cleaned with water and ethanol in an ultrasonic bath before processing. The dimensions of the selected specimens for coating during the structural characterization and electrochemical corrosion test were: 10mm in diameter and 5mm in thickness. Aluminum-Chromium based coatings were deposited by means of an INTERCOVAMEX V3 sputtering system with four magnetrons using DC and pulsed DC power sources, at 50W, from a multicomponent target consisting of Al (99.95% purity), 100mm in diameter and 3mm in thickness) and Cr (99.5% purity). Then the Aluminum and Chromium were sequentially bombarded with argon ions (identification code can be seen in table1). The distance between the erosion target and the substrate was approximately 200mm, 15mm×5mm×1mm) attached to the aluminum target race track. The system was initially pumped to a vacuum pressure of  $1.33 \times 10^{-4}$  Pa. The deposition was done using Ar (99.99% purity) and the pressure in the chamber was  $2 \times 10^{-6}$  Torr. The other deposition parameters were kept constant: the substrate temperature was controlled at 150°C and the Argon flow was kept at 5.8cm<sup>3</sup>/min. The samples deposited on the

substrates were used for structural and morphological characterization by SEM, TEM; AFM, XRD and EIS. The morphological and chemical aspects of the coatings were studied by scanning electron microscopy (SEM/EDS) using a JEOL Model JSM-5800LV.

**Table 1.** Sample code identification

Material (sustrate)	Films (bilayers)	Code
AISI 9840	Aluminum/Chromium	9840 Al/Cr
	Chromium / Aluminum	9840 Cr/Al
AA 6061-T6	Aluminum / Chromium	6061 Al/Cr
	Chromium / Aluminum	6061 Cr/Al
AA 2024-T3	Aluminum / Chromium	2024 Al/Cr
	Chromium / Aluminum	2024 Cr/Al

The structural analysis and thickness were determined by Transmission Electron Microscope in Philips CM200 operated at 200 Kv. The morphological performance of the surface coatings were analyzed by Atomic Force Microscope VEECO Instruments MultiMode IVa. The XRD measurements of the films were performed by a X-ray diffraction, analysis of sintered specimens was performed in a Siemens diffractometer, model D5000, employing Cu Ka1 radiation ( $k = 1.54184 \text{ \AA}$ ), setting up the operating voltage and current at 34 kV and 28 mA, respectively, and the scanning angle range from 10 to 150°. The corrosion behavior of the coated steel and aluminum alloys was determined by electrochemical impedance spectroscopy measurements, an electrochemical interface Solartron SI 1287 and Impedance/Gain Phase Analyzer SI 1287 using a graphite bar as the counter electrode and a saturated calomel electrode (SCE) as reference electrode was employed to perform corrosion experiments. The EIS measurements were carried out in the frequency region from 100,000 to 0.01 Hz (30 frequency points per decade) with amplitude of 10mV rms.

### 3. RESULTS AND DISCUSSION

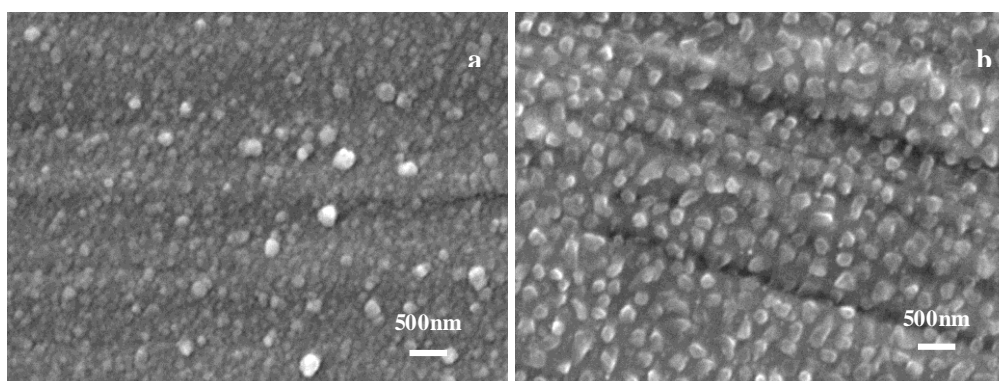


**Figure 1.** Bilayer surface morphology a) Al / Cr b) Cr / Al on steel 9840 at 20.000x.

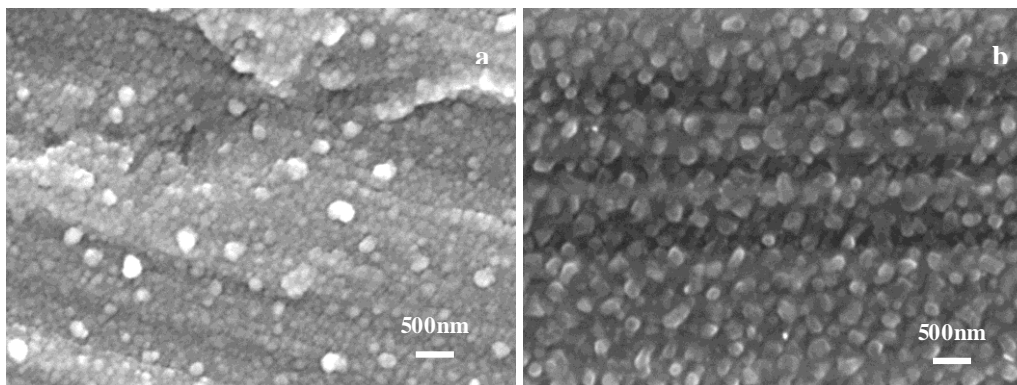


**Figure 2.** Bilayer surface morphology a) Al / Cr b) Cr / Al on AA6061-T6 at 20.000x.

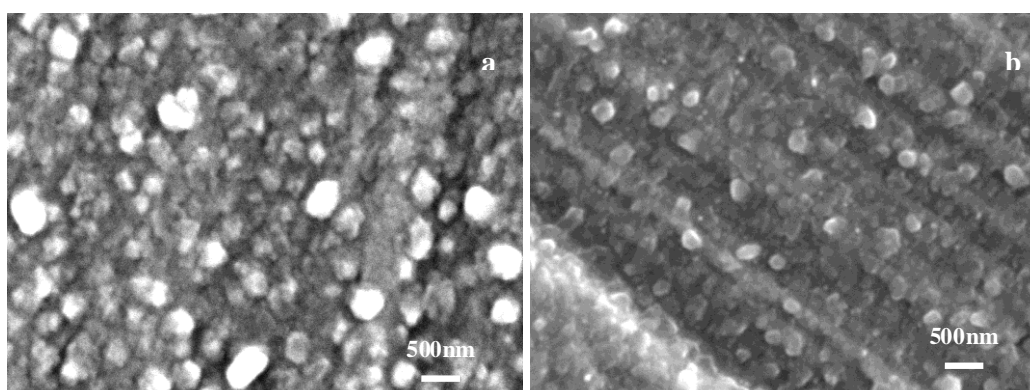


**Figure 3.** Bilayer surface morphology a) Al / Cr b) Cr / Al on AA6061-T6 at 20.000X.

The microstructure of magnetron-sputtered pure Al and Cr coatings was investigated using scanning electron microscopy (SEM- JSM-5800 LV).

Figures 1, 2 and 3 shows the surface of a pure Al and Cr sputter deposits on all substrates. The pure Al and Cr coatings morphology were granular and almost completely featureless which is typical of the dense, non-columnar, coatings which can be deposited by unbalanced magnetron sputtering.

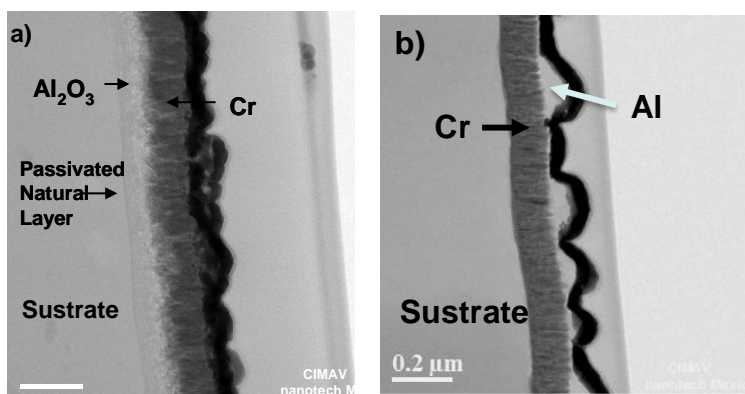


**Figure 4.** Cross-sectional micrographs of magnetron-sputtered of: a) Al/Cr y b) Cr/Al on Aluminum 6061-T6 using TEM.

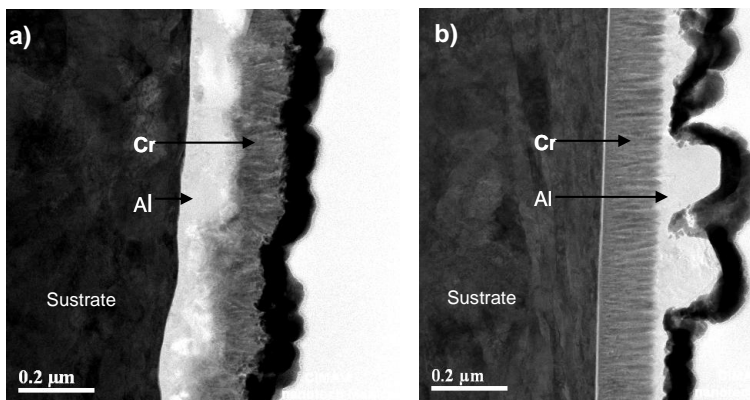


**Figure 5.** Cross-sectional micrographs of magnetron-sputtered of: a) Al/Cr y b) Cr/Al on AISI 9840 Steel using TEM.

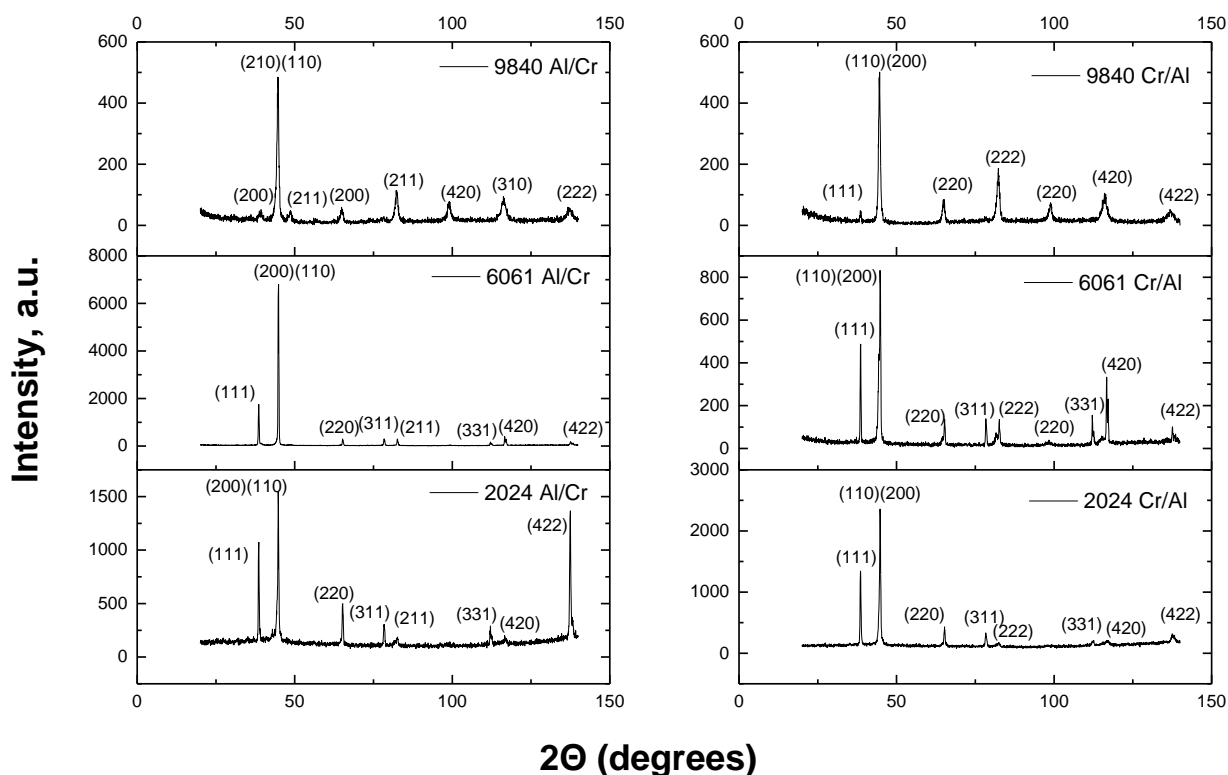


**Figure 6.** X-ray diffraction spectra of different samples without and with bilayers Al-Cr and Cr-Al.

The pure Al and Cr coating appeared to afford complete coverage to the substrate and was almost completely free of holidays (small pores) or other microscopic surface defects. In Al/Cr bilayers there are small particles, but it can be seen a few big particles (figures 1a, 2a and 3a). For Cr/Al bilayers the particle size was homogeneous with a biggest density and the morphology was granular (figures 1b, 2b and 3b).

The cross-sectional micrographs of magnetron-sputtered of pure Al-Cr and Cr-Al coatings were investigated using transmission electron microscopy (TEM). Figure 4a shows the cross-sectional

micrographs of the 6061-Al-Cr system and 6061-Cr-Al system. In the 6061-Al-Cr system, in the substrate-coating interface was observed a natural passivated layer, which has a thickness of 4.5 - 7 nm. Also, the Al layer was oxidized. The Cr layer shows a columnar morphology. In the 6061-Cr-Al system (figure 4b), the bilayer of Cr-Al film shows no oxidation. Figure 5 shows the cross-sectional micrographs of the 9840-Al-Cr system and 9840-Cr-Al system. For 9840 steel substrate, no oxidation was present at the different coating systems. In the pure Al-Cr coating the Al layer was flat and almost completely featureless which is typical of the dense, non-columnar coating [14].

The spectra of X-ray diffraction of the samples with bilayers of Cr/Al peaks were observed corresponding to the planes (110) and (200), showed a much higher intensity and the plane (111) that matches the standard value ( $38.47^\circ$  in  $2\theta$ ) of Al, compared to other planes of lower intensity (see Figure 6). The patterns of the bilayer Al / Cr are shown in Figures 4 and 5, the peak intensity is stronger in the plane Cr (110), which diffracted between  $^\circ 2\theta = 44.10$  is also a strong orientation plane (200). No amorphous phase and crystalline reflections of oxide compounds can be seen from the XRD analysis of the Al-Cr or Cr-Al coatings on any substrates.

### 3.1. Electrochemical Characterization

#### 3.1.1. Impedance Analysis

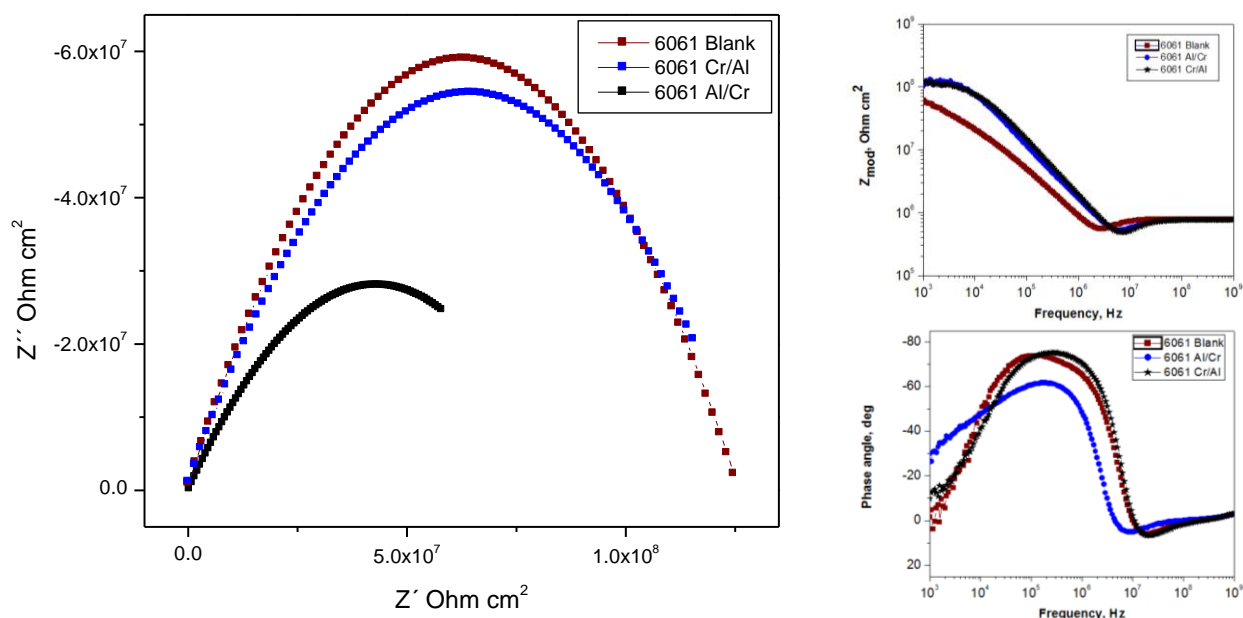


**Figure 7.** Nyquist and Bode diagram for 6061 substrates with bilayers of Cr-Al and Al-Cr in NaCl 3.5% solution.

The impedances of the 6061 alloy with two deposited layers of Al-Cr applied by magnetron sputtering, clearly showed (fig.7) the existence of only one time constant and this is asserted because in the Bode diagram of frequency against phase angle there is a single peak, while in the Nyquist diagram (fig.7) there is only one depressed semicircle which allows to propose an equivalent circuit

which is composed of 2 resistance one due to an electrolyte or solution resistance ( $R_s$ ) and the other resistance due to charge transfer ( $R_{ct}$ ) and a constant phase element (CPE) due to the electrical double layer as an irregular surface which result in a depressed semicircle. This has been previously proposed by a number of investigators [15-17] so the equivalent circuit is shown in figure 10a. The protective properties of the surface in this environment are very similar for 6061 and for the bilayers of Cr-Al coating as reported values for similar load transfer of the order of  $5 \times 10^8 \text{ ohm.cm}^2$ , while the Al-Cr bilayers reports lower values of resistance to charge transfer of about  $6 \times 10^7 \text{ ohm.cm}^2$  which clearly indicates that the electron transfer at the interface is greater.

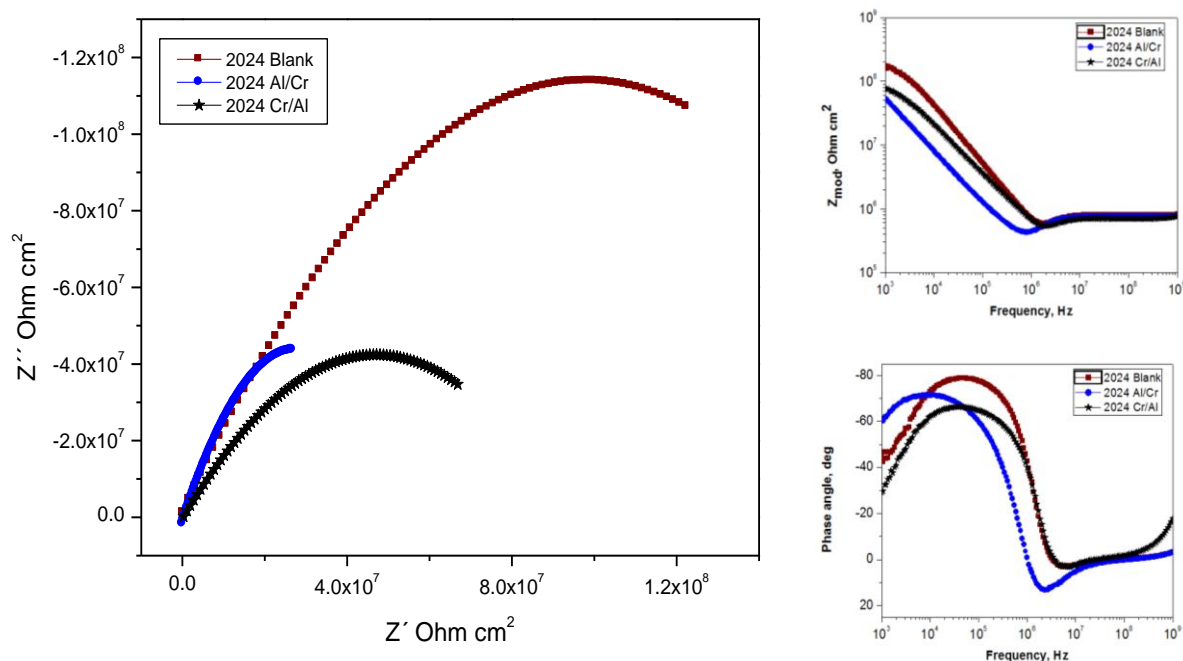


**Figure 8.** Nyquist and Bode diagram for 2024 substrates with bilayers of Cr-Al and Al-Cr in NaCl 3.5% solution.

In the 2024 substrate the impedance diagrams (fig.8) again demonstrate the presence of a single time constant and therefore the same equivalent electrical circuit proposed above. The values of resistance to the charge transfer itself contains the information of how much charge can be accumulated per unit area and how fast it loads and unloads the electrochemical double layer it can be seen major changes in the values of this parameter where blank 2024 reports a high resistance to charge transfer in the order of  $1 \times 10^9 \text{ ohm.cm}^2$ , while layers deposited with Cr-Al reported very similar values as in the previous case, which is a logical circumstance, because the electrochemical phenomena occur on the surface and is evident that in both cases was a similar deposition and therefore achieve similar values.

In 9840 alloys fundamental changes are observed when the material without any deposit, clearly show the existence of only one time constant and this is asserted because in the Bode diagram of frequency against phase angle there is a single peak, while in the Nyquist diagram there is only one

depressed semicircle which allows to propose an equivalent circuit (fig.10b) which is composed of 2 resistance one due to an electrolyte or solution resistance ( $R_s$ ) and the other resistance due to charge transfer ( $R_{ct}$ ) with a value of about  $7 \times 10^7 \text{ ohm.cm}^2$ .

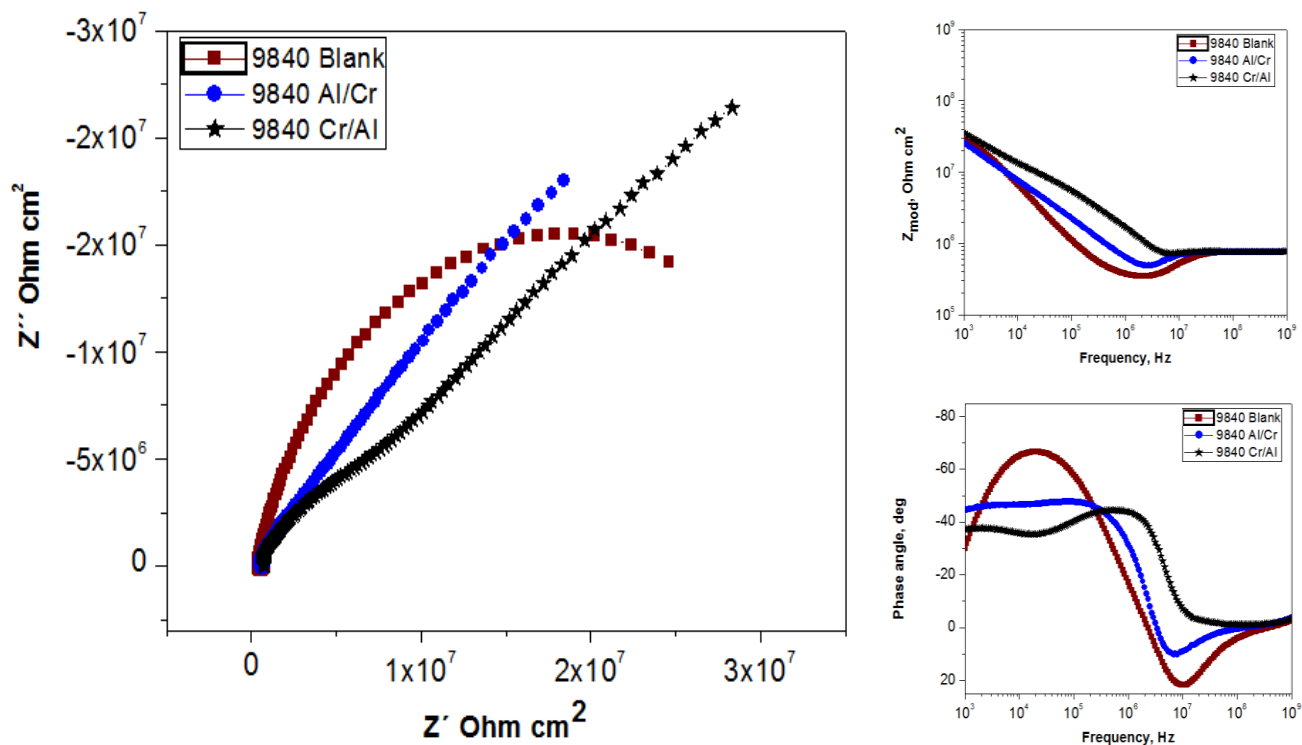


**Figure 9.** Nyquist and Bode diagram for 9840 substrates with bilayers of Cr-Al and Al-Cr in NaCl 3.5% solution.

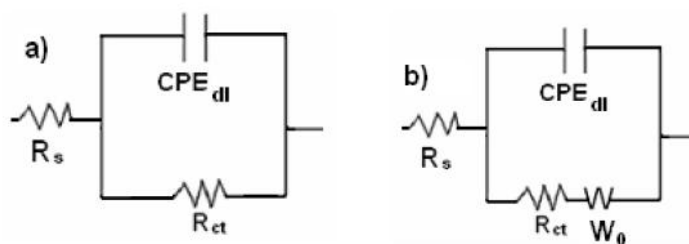


**Figure 10.** Equivalent electric circuits to simulate the EIS results for nanometric Al/Cr and Cr/Al bilayers deposited on AA2024-T3, AA60601-T6 aluminum alloys and AISI 9840 steel by magnetron sputtering exposed to NaCl aqueous solution (3.5 wt %) when the corrosion process is a) under charge transfer control, b) when it is under charge transfer and diffusion control .

However, for the alloy with two deposited layers of Al-Cr and Cr-Al applied by magnetron sputtering, a capacitive-like, depressed semicircle can be observed at high frequencies but at low frequencies both the real and imaginary parts describe a straight line, indicating that the corrosion



process is under a mixed control: by charge transfer at high frequencies, and by diffusion control at low frequencies (fig.9).

#### 4. CONCLUSIONS

The good adhesion, homogeneity and roughness of bilayers depend on the parameters used in deposition. Under the results obtained, it is clear that to both substrates AA2024-T3 and AA60601-T6 aluminum alloys the nanostructured bilayers of Al-Cr are the most stable. Nyquist diagrams show that the aluminum substrates with any bilayer have an activation-controlled process. For the AISI 9840 steel with any nanostructured bilayers have a mixed control by charge transfer at high frequencies, and by diffusion control at low frequencies.

#### ACKNOWLEDGMENTS

This work was supported by Nanomining-263942 (FP7-NMP-2010-EU-MEXICO). The technical assistance by Adan Borunda, Victor Orozco, Enrique Torres, Karla Campos, Oscar Solis and Carlos Ornelas is gratefully acknowledged.

#### References

1. H. Arik, C. Bagci, *Turkish J. Eng. Env. Sci.* 27 (2003) 53–58.
2. H. Schäfer, H.R. Stock, *Corr. Sci.* 47 (2005) 953.
3. W. Kautek, *Corros. Sci.* 28, I73 (1988).
4. J.F. McIntyre and L. Hang, *Corrosion* 50, 26 (1994).
5. J.C. Salvador Fernandes and M.G.S. Ferreira, *Surf Coat. Technol.* 53, 99 (1992).
6. B. Bostan, A.T. Özdemir, A. Kalkanli, *Powder Metall.* 47 (2004) 37–42.
7. M. Bethencourt, F.J. Botana, M.J. Cano, M. Marcos, *Appl. Surf. Sci.* 238 (2004)278.
8. L.E.M. Palomino, J.F. de Castro, I.V. Aoki, H.G. de Melo, *J. Brazil Chem. Soc.* 14 9. (2003) 651.
10. P. Campestrini, H. Terryn, A. Hovestad, J.H.W. Wit, *Surf. Coat. Technol.* 176 11. (2004) 365.
12. M. Dabalà, L. Armelao, A. Buchberger, I. Calliari, *Appl. Surf. Sci.*172 (2001)312.
13. A.E. Hughes, R.J. Taylor, B.R.W. Hinton, L. Wilson, *Surf. Interf. Anal.* 23 (2004)540.
14. F. Mansfeld, Y. Wang, *Appl. Surf. Sci.* 198 (1995) 51.
15. M.A. Domínguez-Crespo, A.M. Torres-Huerta, S.E. Rodil, E. Ramírez-Meneses, G.G. Suárez-Velázquez, M.A. Hernández-Pérez. *Electrochimica Acta* 55 (2009) 498
16. D.P. Monaghan. D.G. Teer, P.A. Logan, K.C. Laing, R.I. Bates and R.D. Amell, *Surf. Coat. Technol.* 60, 592 (1993).
17. D. Risovic, S.M. Poljacek, K. Furic, M. Gojo, *Appl. Surf. Sci.* 255 (2008) 3063.
18. W.H. Mulder, J.H. Sluyters, *Electrochim. Acta* 33 (1988) 303.
19. E. Garcia-Ochoa, J. Genesca, *Surf. Coat. Technol.* 184 (2004) 322.